ARTICLE IN PRESS

Renewable Energy xxx (2014) 1–7

Contents lists available at ScienceDirect

Renewable Energy

journal homepage: www.elsevier.com/locate/renene

Numerical simulation of horizontal tube bundle falling film flow pattern transformation

Jingdong Chen, Ruihang Zhang, Runping Niu*

School of Environment and Energy Engineering, Beijing University of Civil Engineering and Architecture, Beijing 100044, China

ARTICLE INFO

Article history:
Received 22 April 2014
Accepted 1 August 2014
Available online xxx

Keywords:
Horizontal tube bundle
Falling film
Flow pattern

ABSTRACT

It is important to study the falling-film pattern of a horizontal tube bundle in order to set up a heat and mass transfer model accurately. The falling-film pattern of a horizontal tube bundle is simulated in this paper. The technique is based on computational flow dynamics (CFD) for the two-phase flow of gas and water. The experimental results were used to validate the mathematical model. It indicates that the simulation results accord with experimental data well. The simulated results show that the flow pattern varies with different flow rates. Under the different flow rates, it observes the droplet, droplet-columnar, columnar, columnar-sheet and sheet flow patterns. The critical value is 0.0125 kg/s between droplet and columnar, and the critical value is 0.02 kg/s between columnar and sheet.

1. Introduction

Falling film horizontal tube heat exchangers have been widely used in many fields such as refrigeration, chemical engineering, petrochemical processing, the desalination industry and so on [1]. With the development of falling film technology, conventional heat exchangers, such as the coil and flooded heat exchangers, are being replaced gradually since falling film technology has significant advantages. These include: (a) the liquid distributed evenly over the surface of the tube exhibits a minimal differential pressure. Hence, the liquid flow of the pressure drop over the tubes is negligible. (b) The quantity of cooling liquid required for the falling film process is small. (c) The heat transfer coefficients are high. The overall heat transfer coefficients can achieve between 500 w/($m^2 \cdot k$) and 1000 w/($m^2 \cdot k$) [23]. With the increasing application of falling film technology, the resulting transformation of flow patterns by horizontal tube bundles has received wide attention. These flow patterns include droplet, droplet-columnar, columnar, columnar-sheet and sheet. As can be seen from Fig. 1, the different flow patterns are related to multiple factors, such as liquid flow, tube pitch, shape of tube surface, and kinds of refrigerant. The heat and mass transfer areas between liquid and gas vary with the flow pattern on the tube bundle.

Mitrovic reveals that the heat transfer from the heated surface to the liquid film depends not only on the Reynolds Number but also on the tube spacing and the flow pattern [45]. Ganic and Roppo set up an experimental study of the effects of the tube spacing and the liquid film inlet temperature on the breakdown heat flux and heat transfer coefficient [67]. Armbruster and Mitrovic simulated the transformation of the flow pattern based on the equation $Re = AGa^{1/4}$ [see Table 4]. For sufficiently high stagnation pressure, they observed that the radial flows from adjacent jets collide and the film surface among the jets is raised. The crests created at the top of the tube remain nearly unchanged around the tube, and form the departure sites for jets leaving the tube [8]. Based on extensive observations of flow mode transitions, Hu and Jacobi [9] suggested the following flow modes: the droplet mode, the droplet-columnar mode, the columnar mode, the columnar-sheet mode, and the sheet mode. Experiments reported are exploring the viscous, surface tension, inertial, and gravitational effects on the falling-film pattern transitions. Based on this situation, they give a mathematical relationship between Re and Ga ($Re = AGa^b$), where A and b are the empirical constants in the formula, as shown in Table 1 [8].

With the pipe diameter remaining constant, the flow rate is the most important factor for the change of Re. The critical value is tested repeatedly by the numerical simulation method, because of different spray flows leading to the change of flow pattern between tubes. This resulted in the change of contact area between liquid and air, which affects the mass transfer process between liquid and air, and heat transfer between liquid

---

* Corresponding author. Tel.: +86 01068322133; fax: +86 01068322516.
E-mail address: niurunping@bucea.edu.cn (R. Niu).

http://dx.doi.org/10.1016/j.renene.2014.08.007
0960-1481/© 2014 Published by Elsevier Ltd.

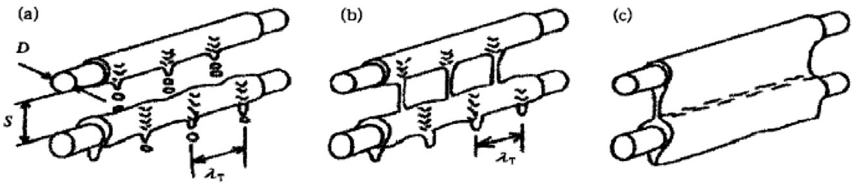

Fig. 1. Horizontal tube bundle falling-film flow pattern (a) droplet (b) columnar (c) sheet. D - pipe diameter; S - tube pitch; λt - Taylor wavelength.

Table 1
The value of A and b[9]

	A	b
Droplet and droplet-columnar	0.074	0.302
Droplet-columnar and columnar	0.096	0.301
Columnar and columnar-sheet	1.414	0.233
Columnar-sheet and sheet	1.448	0.236

Table 3
Simulation result comparison with experiment result.

Flow pattern	Simulation results (kg/s)	Experiment results (kg/s)
Droplet	$Q < 2 \times 10^{-3}$	$Q < 2.1 \times 10^{-3}$
Droplet-column	$2 \times 10^{-3} < Q < 1.25 \times 10^{-2}$	$2.1 \times 10^{-3} < Q < 1.3 \times 10^{-2}$
Column	$1.25 \times 10^{-2} < Q < 1.75 \times 10^{-2}$	$1.3 \times 10^{-2} < Q < 1.7 \times 10^{-2}$
Column-sheet	$1.75 \times 10^{-2} < Q < 2 \times 10^{-2}$	$1.7 \times 10^{-2} < Q < 2.15 \times 10^{-2}$
Sheet	$Q > 2 \times 10^{-2}$	$Q > 2.15 \times 10^{-2}$

and the wall of the tube. So the contact area is supposed to be a factor in calculating the heat-transfer area. The horizontal tube bundle falling-film flow pattern is simulated by the means of computational flow dynamics in this paper.

2. Numerical simulation

2.1. Physical model

The physical model based on Gambit is constructed and a local mesh encryption method is presented. As seen in Fig. 2. The initial parameters are iterated by using Fluent simulation software until convergence, and the accurate calculations are achieved. The arrangement of tubes is staggered, and three tubes form a triangular configuration. The two orifices of the sprayer are on the top of the model and the aperture size is 2 × 2 mm. The flow process of water is adhesive to the walls of the tubes. The flow ranges from 0.0003 kg/s to 0.02 kg/s. As a major objective, the flow pattern is directly influenced by the flow rates, tube pitch and diameter [1].This paper uses water as the simulation liquid. The property parameters are listed, as shown in Table 2. The tube diameter is 14 mm. The tube pitch is 14 mm. The tube is made of copper and has a smooth surface. The model chooses the symmetrical boundary condition. Regardless of water evaporating, the multiphase Volume of Fluid (VOF) model is selected for the simulation based on Fluent simulation software. This model is available for tracking free surface flow. The volume fraction figure shows the film distribution on the wall of the tubes and the flow pattern among the tubes. The volume fraction figure, flow pattern, and falling film volume will vary with flow rate.

2.2. Control equation

The flow field of the tube bundle is described by the following equations.

Continuity equation:

$$\frac{\partial \rho}{\partial t} + \frac{\partial(\rho u)}{\partial x} + \frac{\partial(\rho v)}{\partial y} + \frac{\partial(\rho w)}{\partial z} = 0 \tag{1}$$

$$div(\rho U) = \frac{\partial(\rho u)}{\partial x} + \frac{\partial(\rho v)}{\partial y} + \frac{\partial(\rho w)}{\partial z} \tag{2}$$

where ρ is density in kg/m^3; u is the direction velocity component along the x axis, m/s; v is the direction velocity component along the y axis, m/s; w is the direction velocity component along the z axis, m/s. ‘div’ is called the divergence.

Momentum equation:

$$\frac{\partial(\rho u)}{\partial t} + \frac{\partial(\rho uu)}{\partial x} + \frac{\partial(\rho uv)}{\partial y} + \frac{\partial(\rho wu)}{\partial z} = -\frac{\partial p}{\partial x} + \frac{\partial\left(\mu\left(\frac{\partial u}{\partial x}\right)\right)}{\partial x} + \frac{\partial\left(\mu\left(\frac{\partial u}{\partial y}\right)\right)}{\partial y} + \frac{\partial\left(\mu\left(\frac{\partial u}{\partial z}\right)\right)}{\partial z} + S_u \tag{3}$$

$$\frac{\partial(\rho v)}{\partial t} + \frac{\partial(\rho vu)}{\partial x} + \frac{\partial(\rho vv)}{\partial y} + \frac{\partial(\rho wv)}{\partial z} = -\frac{\partial p}{\partial y} + \frac{\partial\left(\mu\left(\frac{\partial v}{\partial x}\right)\right)}{\partial x} + \frac{\partial\left(\mu\left(\frac{\partial v}{\partial y}\right)\right)}{\partial y} + \frac{\partial\left(\mu\left(\frac{\partial v}{\partial z}\right)\right)}{\partial z} + S_v \tag{4}$$

Table 2
Water properties.

Property parameter	Water
ρ/(kg·m^{-3})	1000
μ/(10^{-3}pa·s)	0.893
C_p/(10^3 kJ kg^{-1} K^{-1})	4.2
σ/(N·m^{-1})	0.07

Table 4
Symbol table.

Symbol	Name	Units
A	Empirical constant	
b	Empirical constant	
ρ	Density	kg·m^{-3}
μ	Dynamic viscosity	10^{-3}pa·s
c_p	Specific heat	103 kJ kg^{-1} K^{-1}
σ	Surface tension	N·m^{-1}
u	Direction velocity component of x axis	m/s
v	Direction velocity component of y axis	m/s
w	Direction velocity component of z axis	m/s
t	Time	s
S	Broader source term	
α	Volume fraction	%
Re	Reynolds number	Dimensionless quantity
Ga	Galileo number	Dimensionless quantity
div	Divergence	

Please cite this article in press as: Chen J, et al., Numerical simulation of horizontal tube bundle falling film flow pattern transformation, Renewable Energy (2014), http://dx.doi.org/10.1016/j.renene.2014.08.007